JOURNAL OF CATALYSIS **172,** 314–321 (1997)
ARTICLE NO. CA971892

Physicochemical Changes in Hydrodesulfurization Catalysts during Oxidative Regeneration

Eun-Suok Oh,* Yong-Chul Park,* In-Chul Lee,†,[1] and Hyun-Ku Rhee*,[2]

*Department of Chemical Engineering, Seoul National University, Kwanak-ku, Seoul 151-742, Korea; and †Korea Institute of Energy Research,
P.O. Box 5, Yousung-ku, Taejeon 305-606, Korea

Received April 28, 1997; revised August 4, 1997; accepted August 26, 1997

Both CoMo and Ni–CoMo catalyst supported over γ-alumina were synthesized and compulsively deactivated by coking from 1,5-hexadiene. The coked catalysts, containing ∼8.8 wt% carbon and ∼7 wt% sulfur, were regenerated by oxidative burnoff at various temperatures in the range of 300–700°C. The catalyst regenerated at each temperature was characterized by various techniques; i.e., BET, XRD, XPS, and TPR. During regeneration, physicochemical properties such as surface area, crystallinity, reducibility, and metal distribution changed significantly with the regeneration temperature. Increase in the dispersion of promoter species (cobalt or nickel) was observed in the catalysts regenerated at low temperatures and this gave rise to the enhancement of activity in comparison to the fresh catalyst. On the other hand, promoters migrated into the sublayer of alumina support at higher temperatures and thus resulted in the formation of $P\mathrm{Al_2O_4}$ ($P =$ Co or Ni) phases. Consequently, the crystallinity of the catalyst increased while the reducibility decreased as the regeneration temperature increased. An abrupt increase in Mo dispersion and a decrease in surface area were observed when the coked catalyst was regenerated at 700°C.

INTRODUCTION

Over the past 30 years a good number of research works on the hydrodesulfurization (HDS) catalysts have been published in the open literature. More specifically, both the nature of active species and the reaction kinetics have been extensively studied and considerable progress has been made in the field while much less attention has been paid to the deactivation and regeneration of HDS catalysts. In recent years, however, some studies on the regeneration of spent catalysts have been motivated due to the reinforced environmental regulations.

HDS catalysts are progressively deactivated in the course of use. The deactivation is primarily due to the coking on the catalyst surface and the deposition of such metals as vanadium, nickel, and iron. Ocampo *et al.* (1) proposed that there were a rapid deposition of coke up to about 25% of the weight of the pellet and a significant decrease of the catalytic activity in the early stage of HDS reaction. They also observed that the catalytic activity decreased more slowly in comparison to the early stage as the reaction time passed. It has been reported by Bogdanor *et al.* (2) that the slow decrease was mainly associated with the deactivation by the metals deposited on the catalyst. Metals in the feedstocks are deposited on the internal and external surfaces of the catalyst and deactivate the catalyst by pore mouth plugging. The deposition of metals is an irreversible process. Tamm *et al.* (3) have reported that the deposited metals poisoned active sites and the poisoning rate was controlled by the diffusion of metal complexes through the pores filled with liquid. Besides these two main causes of catalyst deactivation, HDS catalysts are also deactivated by the agglomeration of active metals and the sintering of support which can occur in the catalyst treated at high temperatures.

In commercial plants a progressive increase in reaction temperature compensates for the continuous decrease of reaction conversion. However, the temperature may be limited by many factors like the product selectivity and the design of units. When it is impossible to increase the reaction temperature due to these factors, the catalyst used in the process is rejected and the operation is shut down immediately. These rejected catalysts can be regenerated by various methods which restore part or all of the original activity.

Oxidative burnoff, one of the more general regeneration methods, can remove the coke deposited on the catalyst surface. And leaching can remove the deposited metals or recover the active metals impregnated in the catalyst. In the case of oxidative burnoff, both coke combustion and oxidation of sulfides liberate significant quantities of heat, which may accelerate the agglomeration of active metals or the sintering of support. Actually, the physicochemical properties of catalyst change during oxidative burnoff whether positively or negatively. For example, the redistribution of active metals, which has a significant effect on the catalytic

---

[1] Deceased.

[2] To whom correspondence should be addressed. E-mail: hkrhee@plaza.snu.ac.kr.

0021-9517/97 $25.00

activity, occurs on the catalyst surface. At high temperature cobalt or nickel migrates from the catalyst surface to the sublayer of the support. Therefore, it is important to control the temperature adequately in the catalyst bed in order to minimize the detrimental effect.

In this study we have two objectives. The first one is to explore what happens to the catalysts during oxidative burnoff. For this purpose, we exposed the CoMo/Al_2O_3 catalyst to coking material and then regenerated the coked catalyst with dry air at various temperatures for a long time. The regenerated catalysts were characterized by X-ray photoelectron spectroscopy (XPS), NO chemisorption, X-ray diffraction (XRD), and temperature programmed reduction (TPR). Here we shall not only elucidate the change in the state of metals with the increase of regeneration temperature but examine its effect on the catalytic activity of thiophene HDS. In addition, the reactivity of carbon and sulfur with oxygen will be examined by temperature-programmed oxidation (TPO). The second objective is to investigate the effect of nickel incorporation to CoMo/Al_2O_3 on both the catalytic activity and the physicochemical properties.

EXPERIMENTAL

Catalysts

The CoMo/Al_2O_3 catalyst was prepared by successive impregnation of ammonium heptamolybdate ($(NH_4)_6 Mo_7O_{24} \cdot 4H_2O$) and cobalt nitrate ($Co(NO_3)_2 \cdot 6H_2O$) solutions onto γ-alumina. After impregnation, the sample was dried with air at 120°C overnight and then calcined at 550°C for 5 h. Its composition was 3.0 wt% CoO and 12.0 wt% MoO_3. A NiCoMo/Al_2O_3 (NiO/CoO = 0.4) catalyst was also synthesized. The aqueous solution of nickel nitrate was brought into contact with the CoMo/Al_2O_3 catalyst calcined at 550°C. The sample containing nickel was treated by the same procedure as mentioned above except for the calcination temperature of 450°C. The BET surface areas of the CoMo/Al_2O_3 and Ni–CoMo/Al_2O_3 catalysts were 194 and 189.8 m^2/g, respectively. For reference, an unpromoted Mo/Al_2O_3 (12 wt% Mo) catalyst was also prepared by impregnation of aqueous ammonium heptamolybdate solution onto γ-alumina support.

Deactivation and Regeneration

The sequential procedure of the regeneration experiment consists of three steps; i.e., sulfidation, deactivation, and regeneration. One gram of the fresh catalyst of 100 to 200 mesh was placed in the fixed-bed microreactor with the quartz filter of 400 mesh. The sample was sulfided at 400°C for 4 h by using the mixture of 35 vol% H_2S in H_2. The total volume of H_2S used for sulfiding was about 10 times of sulfur theoretically required to convert all of metal atoms into sulfided form. The catalyst was then exposed to the constant flow of coking material carried by the nitrogen flow of 425°C. 1,5-hexadiene was used as a coking material and flow lines were heated at 200°C to prevent condensation of the 1,5-hexadiene. Finally, on stopping the flow of coking material, the microreactor was brought to the desired regeneration temperature (300–700°C) and then dry air was introduced into the reactor at the flow rate of 2.4 liters/h for 10 h. After regeneration, the gas stream was switched from dry air to nitrogen and was maintained at the regeneration temperature for 0.5 h. Then, the reactor was cooled down to room temperature.

Activity Testing

In order to compare the activities of the catalysts regenerated at various temperatures, thiophene HDS was conducted at 400°C and atmospheric pressure. Catalyst samples of 100 mg were placed in the reactor with 10 mm I.D. and sulfided at 400°C for 2 h by 15% H_2S/H_2. After the catalyst was sulfided, both hydrogen and thiophene were introduced continuously by using mass flow controller and microfeeder (Sage Instruments syringe pump 341B). The mole ratio of H_2/thiophene was maintained at 20. The feed rate of thiophene was 1.263×10^{-3} mol/hr. Products were analyzed by an on-line G.C. (Hewlett Packard 5890 II) with HP1 capillary column. In the case of thiophene HDS, butene (1-, *cis*-, and *trans*-), butane, and tetrahydrothiophene could be produced. No organic products containing sulfur like tetrahydrothiophene were detected in our study. Therefore, it is reasonable to determine the extent of reaction on the basis of unreacted thiophene.

Characterization

Carbon and sulfur contents of the sample were measured by means of a CHNS analyzer (LECO, CHNS-932). The BET method (Micrometrics Instrument Corporation, ASAP 2000) using N_2 adsorption at −196°C was employed for determining the surface area and the pore volume of the sample. In order to remove physically adsorbed components, the samples were preheated at 300°C for 2 h under helium before N_2 adsorption.

Thermogravimetric analysis (TGA, Perkin-Elmer TGA7) of the deactivated catalyst was performed in air flow. The catalyst sample of 20 mg was heated from 30 to 900°C at the heating rate of 5°C/min. Similarly, the reactivity between the deposited component (C or S) and oxygen was investigated through the TPO experiment. The catalyst sample of 100 mg was passed by the 20 vol% O_2/He mixture and heated to 700°C at the same heating rate as for TGA. A computer connected to a TCD detector (Yanaco 180) monitored periodically the amount of oxygen consumption at an interval of three seconds.

The sample of 100 mg was introduced into the quartz reactor with inner diameter of 10 mm. The sample was slowly heated to the 400°C for 1 h and then cooled to room temperature under pure nitrogen. The sample was then contacted with a gas stream (15 vol% H_2/N_2 mixture, 40 ml/min) and linearly heated to 900°C at the rate of 20°C/min. Water formed during reduction was trapped by molecular sieve 5A at the outlet of reactor. Data acquisition on hydrogen consumption was done by the on-line TCD and computer described above for the TPO experiment.

X-ray photoelectron spectra were obtained by a VSW ESCA Auger system equipped with a monochromatized Al Kα source. All spectra were referenced to the binding energy of oxygen 1s at 531 eV. Before being exposed to the X-ray source in the analysis chamber, the sample crushed and pelletized at high pressure were very slowly heated up to about 200°C by electron beam.

The adsorption of NO on 0.3 g of sulfided sample was measured volumetrically. The sample placed in the U-type pyrex reactor was sulfided at the conditions described in activity testing. Then the whole system was evacuated approximately up to 2×10^{-5} Torr. After these pretreatment, NO uptake measurement was started at room temperature. The gas mixture of 4.97 vol% NO in Ar was introduced at pressures ranging from several to 350 Torr. The amount of NO adsorbed was measured by extrapolating the linear part of the isotherm to zero pressure.

X-ray diffraction (XRD) patterns of the oxidic form of the regenerated catalysts were obtained by means of a Rigaku diffractometer using Cu Kα radiation.

RESULTS

Carbon and Sulfur Removal, Surface Area, and Pore Volume

Carbon and sulfur contents of the coked and regenerated catalysts are summarized in Table 1. Both surface area and pore volume are also listed in the same table. Here CM and NCM represent $CoMo/Al_2O_3$ and $Ni–CoMo/Al_2O_3$, respectively, whereas the number following CM and NCM indicates the regeneration temperature.

The metals impregnated in the catalyst change from oxidic forms to sulfided forms by presulfidation. The metal sulfides can be transformed again by oxidative regeneration into metal oxides. From the sulfur and carbon contents listed in Table 1, we notice that most of the sulfur existing as metal sulfides can be removed at the regeneration temperature (T_r) of 400°C and only a little amount of sulfur remains in the catalyst regenerated at 500°C, while the carbon deposited on the catalyst surface is almost completely removed at $T_r = 400$°C.

In order to find out more accurately the temperature of removal of both carbon and sulfur, TPO experiments were carried out and the corresponding profiles are shown in Fig. 1. There are two peaks for oxygen consumption at 270 and 405°C over the $Ni–CoMo/Al_2O_3$ catalyst presulfided and then coked (Fig. 1a). These peaks are associated with oxygen consumed to convert metal sulfides to metal oxides and to oxidize carbon deposited. In the case of the catalyst directly coked, only one peak appears, corresponding to the position of the second signal of Fig. 1a. Over the sulfided catalyst without coking, two separate peaks slightly overlapped are observed in the low temperature region below 330°C, although we shall not look into the detailed nature for each peak. With respect to the TPO profiles over the sulfided $NiMo/Al_2O_3$, Silva *et al.* (5) reported that the region between 184 and 380°C corresponded to the oxidation of MoS_2 and NiMoS phases. Similar result over the sulfided $CoMo/Al_2O_3$ was given by van Doorn *et al.* (6).

TABLE 1

Carbon and Sulfur Contents and Physical Properties of the Fresh, Coked, and Regenerated Catalysts

Catalyst	Carbon content (wt%)	Sulfur content (wt%)	BET surface area (m^2/g)	Average pore diameter (Å)	Cumulative pore volume (cm^3/g)
CM-fresh	—	—	194.0	103.4	0.507
CM-coked	8.78	7.18	176.7	74.04	0.335
CM-300	4.18	2.16	196.8	85.07	0.427
CM-400	0	0.54	206.6	99.09	0.519
CM-500	0	0.27	206.5	99.30	0.520
CM-600	0	0	205.8	98.12	0.512
CM-700	0	0	153.8	139.3	0.540
NCM-fresh	—	—	189.8	105.2	0.505
NCM-coked	8.78	6.46	178.9	70.06	0.332
NCM-300	4.38	1.81	193.1	85.66	0.421
NCM-400	0	0.38	195.9	101.8	0.505
NCM-500	0	0.27	194.3	103.9	0.511
NCM-600	0	0	199.0	101.2	0.510
NCM-700	0	0	164.0	124.2	0.514

Note. CM ~ $CoMo/Al_2O_3$; NCM ~ $Ni–CoMo/Al_2O_3$. The number following CM or NCM represents the regeneration temperature.

In Fig. 2 the TGA diagram of the coked $Ni–CoMo/Al_2O_3$ catalyst is presented. Approximately 20 wt% of the coked sample is lost when the temperature reaches 700°C. For the derivative of the weight loss, broad or sharp peaks

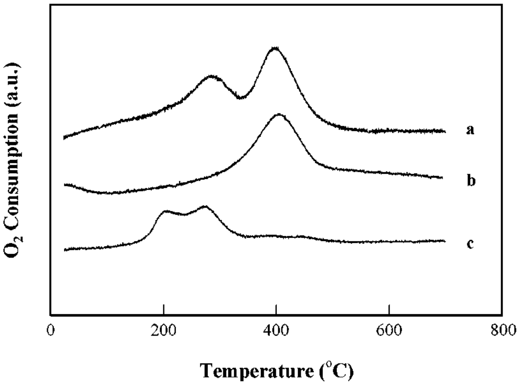

FIG. 1. TPO profiles of the $Ni–CoMo/Al_2O_3$ catalyst: (a) presulfided and then coked; (b) directly coked; and (c) presulfided, respectively.

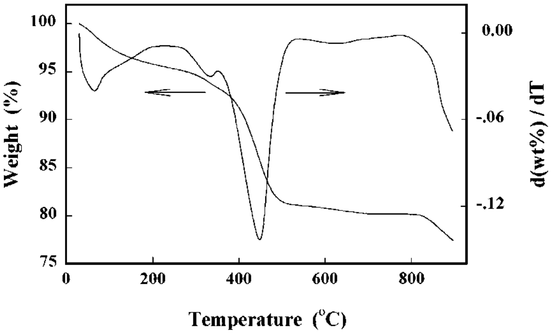

FIG. 2. TGA/DTG diagram of the coked Ni–CoMo/Al_2O_3 catalyst.

occur in five regions; i.e., 50–200°C, 250–350°C, 350–530°C, 550–650°C, and >805°C. At the lowest temperature region (50–200°C), the weight loss results from vaporizing water physically adsorbed on the catalyst. Two peaks corresponding to the transformation of metal sulfides and the removal of carbon are sequentially observed with increase in the temperature. Here the range of 250–350°C shows a small signal for oxygen consumption when compared to the range of 350–530°C, although the coked catalyst contains 6.46 wt% S and 8.79 wt% C. The reason for this is as follows: all of carbon deposited are completely removed while sulfur existing as metal sulfides is removed and simultaneously replaced by oxygen; for example, MoS_2 and Co_9S_8 are converted into MoO_3 and CoO, respectively. Therefore, the weight loss by the oxidation of metal sulfides is much smaller than that by carbon combustion.

Relatively small weight loss is also observed at higher temperature range of 550–650°C. A careful observation on sulfur content summarized in Table 1 reveals that NCM-500 contains only 0.27 wt% sulfur while NCM-600 catalyst contains no sulfur at all. Accordingly, it may be presumed that the weight loss is attributed to decomposition of sulfur-containing compounds. Trimm (7) proposed the following reversible reaction;

$$SO_3 + Al_2O_3 = Al_2(SO_4)_3$$

which can occur during the oxidative regeneration period. Also, he reported that the production of aluminum sulfate was favoured at temperatures below ca. 450°C and reversed above ca. 500°C.

Concerning the BET surface area of the regenerated catalysts given in Table 1, there is a slight increase after the catalyst is oxidized at successively higher temperatures except for 700°C. However, the surface area of the CM-700 (or NCM-700) catalyst is observed to be much smaller than any other regenerated catalysts.

Crystallinity of the Regenerated Catalyst

Figure 3 shows the XRD patterns of the fresh and regenerated catalysts. In the case of nonpromoted catalyst (Mo/Al_2O_3 marked as M-fresh), the peak assigned to well-crystallized MoO_3 is observed at $2\theta = 23.3$ (8). However, the promoted sample (CM-fresh or NCM-fresh) does not show that peak. This suggests that the interaction between promoter (Co or Ni) and Mo increases Mo dispersion affecting considerably the catalytic activity for the HDS reaction.

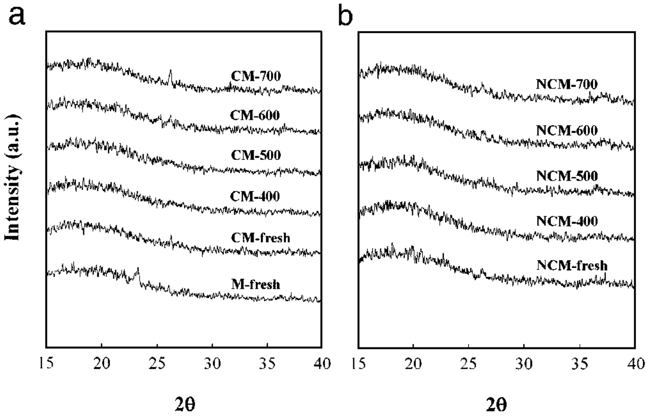

FIG. 3. XRD patterns of the fresh catalyst and the regenerated catalysts: (a) CoMo/Al_2O_3 and (b) Ni–CoMo/Al_2O_3.

The XRD peak at $2\theta = 26.3$ becomes larger as the regeneration temperature increases. Especially, the catalyst regenerated at 700°C produces a significant peak at this diffraction angle. Some authors (8, 9) reported that this reflection corresponded to the hydrated promoter molybdate compound xPO–MoO_3–yH_2O ($P =$ Co or Ni). In the study of oxidic NiMo catalyst, however, Brito *et al.* (10) have shown that this peak was related to the presence of crystalline β-$NiMoO_4$ phase. This peak can be attributed not only to β-$NiMoO_4$ but also to β-$CoMoO_4$ because β-$PMoO_4$ compounds ($P =$ Co or Ni) show almost indistinguishable powder XRD traces (11).

In order to investigate more accurately the nature of this reflection, the coked Mo/Al_2O_3 catalyst (12 wt% MoO_3) is oxidized at 700°C, and the XRD pattern of the regenerated sample is shown and compared to that of CM-700 in Fig. 4.

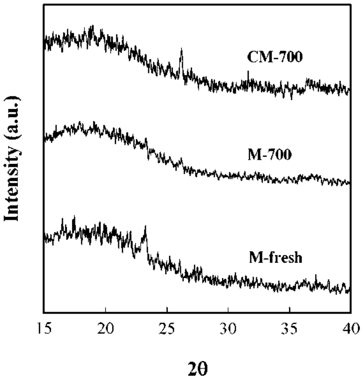

FIG. 4. Comparison of XRD patterns among the fresh Mo/Al_2O_3 catalyst, the regenerated Mo/Al_2O_3 catalyst, and the regenerated CoMo/Al_2O_3 catalyst.

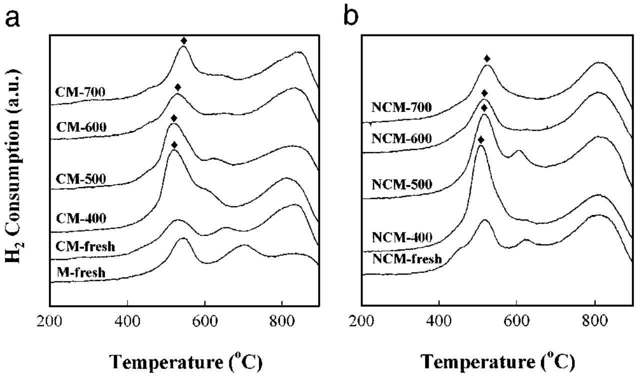

FIG. 5. TPR profiles of the regenerated catalysts: (a) $CoMo/Al_2O_3$ catalyst; (b) $Ni–CoMo/Al_2O_3$ catalyst.

The $2\theta = 26.3$ peak observed in the CM-700 catalyst is not present in the M-700 catalyst.

Reducibility of the Regenerated Catalysts

TPR profiles of the regenerated catalysts are displayed in Fig. 5. Most of the samples studied show three hydrogen consumption regions slightly overlapped; i.e., 400–620°C, 580–720°C, and >700°C. However, there are some differences in the amount of hydrogen consumption and in the temperature of peak maximum (T_{rm}).

In the studies on the reducibility of Mo/Al_2O_3 catalyst (12, 13), the lowest temperature region has been assigned to partial reduction of very dispersed polymolybdate-like species. The highest temperature region has been related to the continued reduction of polymolybdate species plus the reduction of tetrahedrally coordinated molybdate groups interacting more strongly with the support. Laine *et al.* (8) proposed that the reduction in the middle temperature region was shown in the catalyst calcined at high temperature of 600°C and associated with the reduction of bulk MoO_3. It can be confirmed by FT-IR result (14) that polymolybdate is reduced more easily than bulk MoO_3.

On the other hand, Co incorporation in the Mo/Al_2O_3 catalyst only shifts the second peak maximum to lower temperature. Unlike this, Ni incorporation in the $CoMo/Al_2O_3$ catalyst not only makes the TPR peaks sharper but shifts the T_{rm} of each peak to a lower temperature.

In regard to the reducibility of the regenerated CM catalysts in Fig. 5a, it is found that the catalyst regenerated at 400°C shows much larger hydrogen consumption and lower T_{rm} of the second peak compared to the fresh catalyst. In the case of the regenerated NCM catalysts, a similar behavior is observed at 500°C as well as 400°C. However, both of the catalysts show that hydrogen consumption decreases again and the T_{rm}'s of the first and second peaks increase progressively with increasing T_r.

Surface Characterization of the Regenerated Catalyst

XPS is one of the most powerful methods to obtain information on the elemental composition, the oxidation state of the elements, and the metal dispersion. In Fig. 6 XPS spectra on each atom of the regenerated NCM catalysts are presented. The $Mo_{3d_{5/2,3/2}}$ doublet of Mo^{6+} ions are shown at 232.8 and 235.6 eV. In comparison to the fresh catalyst, there is no noticeable difference in both the peak position and the peak intensity when the coked catalyst is regenerated at less than 600°C. However, an abrupt increase in the peak intensity is observed in the catalyst regenerated at 700°C. This is a factor of about 3 by contrast with the fresh catalyst. If the peak intensity is calculated with the ratio of Mo_{3d}/Al_{2p}, the difference between NCM-fresh and NCM-700 becomes even larger because the Al_{2p} intensity of NCM-700 is lower than that of NCM-fresh.

In the cases of Co and Ni used as promoters, the characteristic peaks of $Co_{2p_{3/2,1/2}}$ and $Ni_{2p_{3/2,1/2}}$ are shown at 781.7, 797.5 eV and 855.9, 873.7 eV, respectively. Besides, shake-up satellites which are typically observed for the $2p$ levels of transition metals with unpaired d electrons are also shown in the XPS spectra of both ions, although it is very difficult to decide the accurate positions of the satellite peaks due to the noise of the spectra by a small amount of metals.

To obtain more detailed information on the redistribution of metals, NO chemisorption was carried out and the

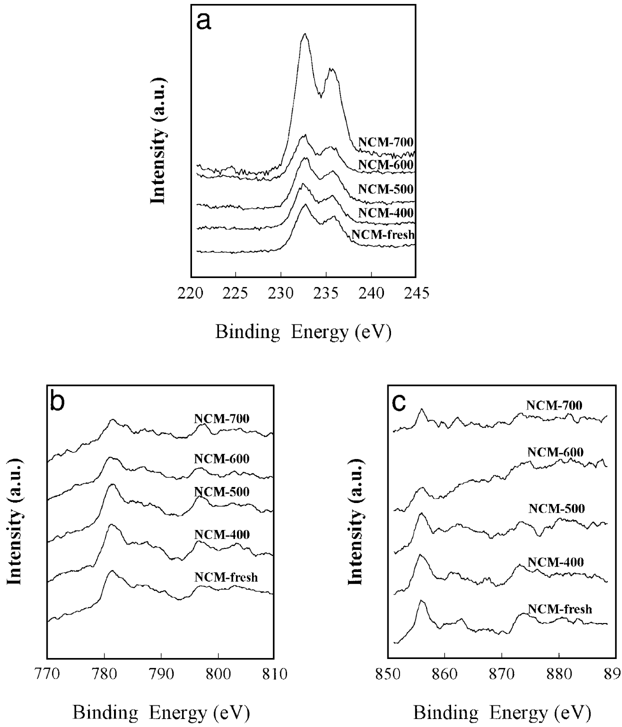

FIG. 6. XPS spectra of the regenerated $Ni–CoMo/Al_2O_3$ catalysts: (a) Mo_{3d}; (b) Co_{2p}; and (c) Ni_{2p}.

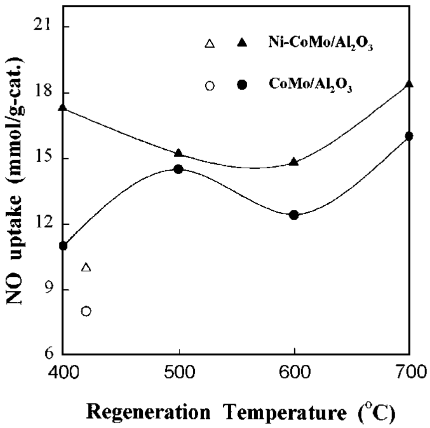

FIG. 7. NO uptake of the regenerated catalysts (open: fresh catalyst; solid: regenerated catalyst).

results are shown in Fig. 7. Regardless of the regeneration temperature, the regenerated catalysts adsorb NO more abundantly than the fresh catalyst. NO uptake increases with increasing T_r when the coked CM catalyst is regenerated at temperatures below 500°C. However, the CM catalyst regenerated at 600°C shows smaller NO uptake than the CM-500 catalyst.

A dissimilar tendency to the CM catalyst is shown in NO uptake data of the NCM catalysts. The NCM-400 catalyst shows the largest NO uptake of all catalysts regenerated at temperatures below 600°C. On the other hand, there is a noticeable increase in the amount of NO adsorbed in both catalysts regenerated at 700°C.

Activity of the Regenerated Catalysts

As shown in Fig. 8 and Table 2, the regeneration temperature has a considerable effect on the catalytic activity. The activity depends strongly on physicochemical properties, which vary according to the regeneration temperature. In particular, it has been known that the distribution of active metals on the catalyst surface is one of the most important factors dominating the activity and that there is an optimum Promoter/Mo ratio for HDS activity.

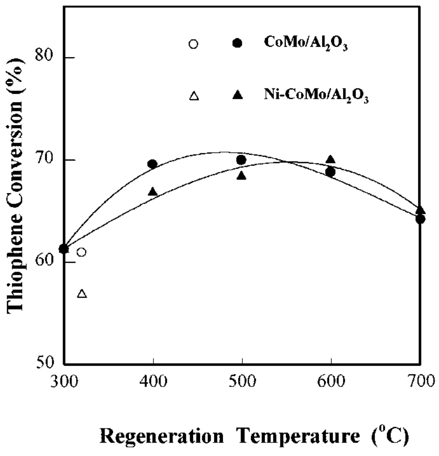

FIG. 8. Effect of the regeneration temperature on the catalytic activity for thiophene HDS at 400°C over CoMo/Al$_2$O$_3$ and Ni–CoMo/Al$_2$O$_3$ catalysts, respectively (open: fresh catalyst; solid: regenerated catalyst).

TABLE 2

Activity and Turnover Frequency for Thiophene HDS over Fresh and Regenerated Catalysts

Regeneration temp. (°C)	Activity (μmol/s · g-cat)		TOF (s^{-1})	
	CM	NCM	CM	NCM
300	2.15	2.15	—	—
400	2.44	2.34	2.88	1.76
500	2.45	2.40	2.20	2.05
600	2.39	2.45	2.50	2.16
700	2.25	2.28	1.80	1.58
Fresh	2.13	2.00	3.53	2.81

In the case of the regenerated catalysts, the CM catalysts regenerated at 400°C show higher activity (or turnover frequency) than any other catalysts regenerated at different temperatures while the regenerated NCM catalyst shows the highest activity (or turnover frequency) at the regeneration temperature of 600°C. The catalysts regenerated at 300°C show very low activity due to the incomplete removal of the deposited carbon. It is also seen that the CM-700 (or NCM-700) catalyst is less active than the CM (or NCM) catalyst regenerated at different temperatures except for 300°C.

DISCUSSION

From the TPO profiles in Fig. 1, it is evident that the oxidation of metal sulfides is accomplished at lower temperature than that of carbon deposited during oxidative regeneration. Approximately, the oxidation at 400°C can remove almost all of the sulfur and carbon deposited on the catalyst surface. However, some of the sulfur compounds are more refractory than carbon and removed at a temperature higher than $T_r = 500$°C. These may be sulfur-containing compounds like aluminum sulfate ($Al_2(SO_4)_3$) combined strongly with alumina support.

The BET results of the regenerated catalysts reveal that there is a substantial decrease in the surface area of the catalyst regenerated at 700°C. In general, it has been understood that alumina has stable hydroxyl groups on the surface such as −OH and $-OH_2$ and that the groups can be removed when exposed to high temperatures for a long time. Therefore, the substantial decrease may be due to the structural change of alumina support by dehydration and removal of hydroxyl groups. According to the previous works (15, 16), on the other hand, loss of MoO_3 by sublimation was observed during regeneration or during simple heating in air at temperatures as high as 800°C but in the presence of steam at lower temperatures. Accordingly, the weight loss in the highest temperature range in TGA diagram of Fig. 2 corresponds to the sublimation of MoO_3.

By comparing the XRD patterns between M-700 and CM-700 in Fig. 4, it is noticed that the growth of peak intensity at $2\theta = 26.3$ is mainly associated with an increase in crystallinity of the compound related to the promoter (Co or Ni), though the compound may be either the hydrated promoter molybdate or a compound like β-PMoO$_4$. Also, the XRD pattern of the M-700 catalyst indicates a possibility on the increase of Mo dispersion since the $2\theta = 23.3$ peak shown in the fresh Mo/Al_2O_3 catalyst is not identified in the M-700 catalyst. Compared to the regenerated CM catalyst, the regenerated NCM catalyst is observed to show a remarkable growth of the XRD peak at $2\theta = 37.1$ (Fig. 3). This suggests that Ni spinel ($NiAl_2O_4$) phase is formed at high temperatures by the migration of Ni atoms into the sublayer of the support.

As shown in Fig. 5, the reducibility of the catalyst is significantly affected by the regeneration temperature. The enhancement of reducibility by regeneration at relatively low temperatures indicates an indirect proof on the redistribution of promoter ions (Co and Ni); namely, a new interaction between the redistributed promoter ion and Mo enhances the reducibility of Mo. Maybe the redistribution results from the oxidation of carbon and metal sulfides. On the other hand, the hydrogen consumption decreases and T_{rm} increases probably due to the formation of species like P spinel ($P = \mathrm{Co}$ or Ni) which are not reduced easily.

According to Arteaga *et al.* (16, 17), redistribution of Mo atoms has been observed at high temperatures during oxidation of MoS_2 crystallites. These authors reported that this was due to the high mobility of MoO_3. Thus, a significant increase in the Mo_{3d} intensity of Fig. 6 can be explained by the following arguments; MoO_3 generated by decomposition of the promoted polymolybdate structures sublimes from within the porous structure to the external surface of the particles or to MoO_3-free area of the support as indicated by the authors. Hence, the dispersion of Mo^{6+} ions on the catalyst surface increases. This is a parallel result with Mo/Al_2O_3 XRD shown in Fig. 4.

Unlike Mo ions, the XPS peak intensity of Co and Ni ions tends to decrease as the regeneration temperature increases. This provides a good insight into the diffusion of Co and Ni ions. The promoter ions migrate from the surface to the sublayer of alumina and consequently the peak area decreases. The migrated promoter ions form spinel species with alumina.

From the NO uptake results, it may be concluded that the redistribution of Co atoms by low-temperature regeneration at 400–500°C provides more active sites which are probably related to Co atoms interacting with Mo atoms. On the other hand, the higher temperature regeneration brings about not only the redistribution of Co atoms on the catalyst surface but the migration of Co atoms into the sublayer of the support and, hence, the amount of Co atoms existing on the surface decreases and this leads to the decrease of NO uptake. In the case of Ni atoms, the Ni-related sites which can adsorb NO molecules may be very stable at low temperatures of 400°C but easily broken at higher temperatures. In addition, Ni migrates into the support matrix at lower temperature than Co. Consequently, the NO uptake of the NCM-500 catalyst decreases despite the increase of Co-related sites at 500°C when compared to that of the NCM-400 catalyst.

On the other hand, there is a noticeable increase in the amount of NO adsorbed in both catalysts (CM-700 and NCM-700). Probably the increase of nonpromoted-Mo sites on the catalyst surface, a good accordance with XPS spectrum of NCM-700, gives rise to increasing NO uptake despite the decrease of Co- and Ni-sites.

From the comparison of the activity between CM-fresh and NCM-fresh catalysts, it is clear that Ni addition affects negatively the catalytic activity for thiophene HDS. This is understood to be caused by the deviation of the optimum promoter/Mo ratio; namely, the increase of atomic ratio by Ni addition leads to decrease in thiophene HDS activity.

As confirmed by various characterization methods, the redistribution of promoter ions occurs during regeneration; for instance, Co or Ni dispersion increases at low regeneration temperature. Such increase of Co dispersion in the CM catalyst affects positively the catalytic activity of thiophene HDS. Like the unfavorable effect of Ni addition, however, the increase of Ni dispersion acts negatively rather than positively. Therefore, it is speculated that the migration of Ni atoms into alumina support gives rise to the optimum promoter/Mo ratio for higher thiophene HDS activity and thus minimizes the negative effect on thiophene HDS. Consequently, the NCM catalyst regenerated at higher temperature (NCM-600 catalyst) shows the highest activity.

When the coked catalyst is regenerated at 700°C, the dispersion of Mo atoms increases but the promoters diffuse into alumina support. Accordingly, the possibility to form the interaction phases between promoters and Mo may become weak, which results in the decrease of the catalytic activity for thiophene HDS. In addition, the decrease of surface area can provide another cause for the decrease of the activity.

The fresh catalysts have higher TOF than the regenerated ones because there exist relatively few sites adsorbed by NO on the catalyst surface. The CM-400 catalyst shows the highest TOF among the regenerated catalysts because of the lowest amount of NO adsorbed and the highest activity. On the other hand, as the regeneration temperature increases, the amount of NO adsorbed decreases due to the migration of promoter atoms, whereas rather small changes are observed in the catalytic activity. Hence, the TOF gradually increases. At the highest regeneration temperature, i.e., 700°C, however, only an extremely small number of promoter atoms remain on the catalyst surface, so most of the Mo sites become unpromoted. Therefore, the TOF value is considerably lowered.

CONCLUSIONS

From the results of TPO and CHNS analyses, it is concluded that carbon and sulfur deposited on the catalyst surface can be removed at the regeneration temperatures above 400°C. Here, metal sulfides react with oxygen more readily than the deposited carbon. When the coked catalysts were regenerated at temperatures below 600°C, neither the surface area nor the pore volume of the regenerated catalysts changed significantly, compared to the fresh catalyst. However, long time exposure at a high temperature produced both the dehydration of alumina and the sublimation of MoO_3 and consequently resulted in the significant decrease of surface area and the weight loss.

The redistribution of promoters (Co and Ni) occurred on the catalyst at a relatively low regeneration temperature. This gave rise to an enhancement of the catalytic activity for the hydrodesulfurization of thiophene. This redistribution of metals on the surface is probably attributed to the oxidation of metal sulfides and the deposited carbon. In the case of Mo, the dispersion increased abruptly at the regeneration temperature of 700°C. Despite the increase of Mo dispersion, however, the activity is observed to decrease because of other detrimental effects such as the decrease in both the surface concentration of the promoter ion and surface area.

As the regeneration temperature increased, promoters migrated progressively from the surface to the sublayer of the support and formed the inactive $P\mathrm{Al}_2\mathrm{O}_4$ phase (P for Co or Ni) with the alumina. Finally, the P/Mo ratio on the surface changed and this change exerted a dominant influence on the activity of the regenerated catalysts for thiophene HDS.

REFERENCES

1. Ocampo, A., Schrodt, J. T., and Kovach, S. M., *Ind. Eng. Chem. Prod. Des. Dev.* **17**, 56 (1978).
2. Bogdanor, J. M., and Rase, H. R., *Ind. Eng. Chem. Prod. Dev.* **25**, 220 (1986).
3. Tamm, P. W., Harnsberger, H. F., and Bridge, A. B., *Ind. Eng. Chem. Proc. Des. Dev.* **20**, 262 (1981).
4. Yoshimura, Y., and Furimsky, E., *Appl. Catal.* **23**, 157 (1986).
5. Teixeira da Silva, V. L. S., Frety, R., and Schmal, M., *Ind. Eng. Chem. Res.* **33**, 1692 (1994).
6. van Doorn, J., Bosch, J. L., Bakkum, R. J., and Moulijn, J. A., "Catalyst Deactivation," p. 391. Elsevier, Amsterdam, 1987.
7. Trimm, D. L., "Catalysis in Petroleum Refining 1989," p. 41. Elsevier, Amsterdam, 1990.
8. Laine, J., Brito, J. L., and Severino, F., *J. Catal.* **131**, 385 (1991).
9. Madeley, R. A., and Wanke, S. E., *Appl. Catal.* **39**, 295 (1988).
10. Brito, J. L., and Laine, J., *Appl. Catal.* **72**, L13 (1991).
11. Rob van Veen, J. A., Gerkema, E., van der Kraan, A. D., Hendriks, P. A. J. M., and Beens, H., *J. Catal.* **133**, 112 (1992).
12. Arnoldy, P., Franken, M. C., Scheffer, B., and Moulijn, J. A., *J. Catal.* **96**, 381 (1985).
13. Brito, J. L., and Laine, J., *J. Catal.* **139**, 540 (1993).
14. Seyedmonir, S. R., Abdo, S., and Howe, R. F., *J. Phys. Chem.* **85**, 1233 (1982).
15. Stanislaus, A., and Al-Dolama, K., *J. Catal.* **101**, 536 (1986).
16. Arteaga, A., Fierro, J. L. G., Grange, P., and Delmon, B., *Appl. Catal.* **34**, 89 (1987).
17. Arteaga, A., Fierro, J. L. G., Grange, P., and Delmon, B., *in* "Catalyst Deactivation" (B. Delmon and G. F. Forment, Eds.), p. 59. Elsevier, Amsterdam, 1987.